Anti-Inflammatory Effects of Sulfatide in Macrophage through Inhibition of HMGB1 Secretion

Hee Sue Kim

Department of Medicine or Medical Science

The Graduate School, Yonsei University

Anti-Inflammatory Effects of Sulfatide in Macrophage through Inhibition of HMGB1 Secretion

Hee Sue Kim

Department of Medicine or Medical Science

The Graduate School, Yonsei University

Anti-Inflammatory Effects of Sulfatide in Macrophage through Inhibition of HMGB1 Secretion

Directed by Professor Jeon-Soo Shin

The Doctoral Dissertation
submitted to the Department of Medical Science,
the Graduate School of Yonsei University
in partial fulfillment of the requirements for the degree
of Doctor of Philosophy

Hee Sue Kim

December 2020

This certifies that the Doctoral Dissertation
of Hee Sue Kim is approved.

Thesis Supervisor : Jeon-Soo Shin

Thesis Committee Member : Je-Wook Yu

Thesis Committee Member : Kyung-Hee Chun

Thesis Committee Member : Sang Ho Oh

Thesis Committee Member : Jun-Young Seo

The Graduate School
Yonsei University

December 2020

TABLE OF CONTENTS

LIST OF FIGURES

Anti-Inflammatory Effects of Sulfatide in Macrophage through Inhibition of HMGB1 Secretion

Hee Sue Kim

Department of Medicine or Medical Science
The Graduate School, Yonsei University

(Directed by Professor Jeon-Soo Shin)

The high mobility group box 1 (HMGB1) is a well-known late mediator of sepsis secreted by multiple stimuli. Such stimuli involve multiple pathways, such as the mitogen-activated protein kinase (MAPK) and nuclear factor kappa B (NF-κB) pathways, and reactive oxygen species (ROS) under inflammation. Sulfatide, on the other hand, is a sphingolipid commonly found in myelin sheets with a disputed immunological role where it is reported to be pro-inflammatory in the central nervous system, whereas it shows protective effect in the periphery. Such discrepancy regarding the immunological characteristics of sulfatide led me to seek to determine the immunological characteristics of sulfatide in the periphery. Immunological characteristics of sulfatide was analyzed through studying the secretion of HMGB1 triggered by lipopolysaccharide (LPS) stimulation in Raw 264.7 cells after pre-treatment or post-treatment of sulfatide. Suppression of HMGB1 secretion by inhibiting its cytosolic translocation was observed after both pre-treatment with sulfatide before LPS stimulation, and post-treatment with sulfatide after LPS stimulation. Further analysis of the downstream molecules of toll-like receptor (TLR) signaling revealed suppression of c-Jun N-terminal kinase (JNK) phosphorylation and p65 translocation. LPS-mediated ROS production was also decreased when sulfatide pre-treatment was provided, caused by the down-regulation of the phosphorylation of activators, such as IRAK4 and TBK1. Investigation of the upstream mechanism that encompasses all the aforementioned inhibitory characteristics unveiled the involvement of lipid rafts. In addition to the co-localization of biotinylated sulfatide and monosialotetrahexosylganglioside, a decrease in LPS-induced co-localization of TLR4 and lipid raft markers was observed when

sulfatide treatment was given before LPS stimulation. Overall, pre-treated sulfatide was found to exert its anti-inflammatory properties by hindering the co-localization of TLR4 and lipid rafts, nullifying the effect of LPS on TLR4 signaling. On the other hand, post-treatment of sulfatide exhibited anti-inflammatory characteristics via modifying metabolic characteristics of macrophage. Similar effects of sulfatide were also confirmed in the LPS-mediated murine experimental sepsis model, showing decreased levels of serum HMGB1, TNF-α, IL-6, increased survivability, and reduced pathological severity.

List of Abbreviations

BCA	Bicinchoninic Acid	**LBP**	LPS Binding Protein
BSA	Bovine Serum Albumin	**LPS**	Lipopolysaccharide
CD14	Cluster of Differentiation 14	**MAPK**	Mitogen-activated Protein Kinase
CD1d	Cluster of Differentiation 1d	**MD2**	Myeloid Differentiation 2
CXCL12	C-X-C motif ligand 12	**MEM**	Minimum Essential Medium
DAMP	Danger Associated Molecular Pattern	**NF-κB**	Nuclear factor-κB
DAPI	4′,6-diamidino-2-phenylindole	**NKT cell**	Natural Killer T cell
DNA	Deoxyribonucleic acid	**OCR**	Oxygen Consumption Rate
ECAR	Extracellular Acidification Rate	**PBS**	Phosphate Buffered Saline
ELISA	Enzyme-linked Immunosorbent Assay	**RIPA**	Radioimmunoprecipitation Assay
ERK	Extracellular signal-regulated kinase	**ROS**	Reactive Oxygen Species
HMGB1	High Mobility Group Box 1	**TBK1**	TANK-binding Kinase 1
IκBα	Inhibitor of Kappa Light Chain Gene Enhancer in B Cells, Alpha	**TCA**	Trichloroacetic acid
IL-6	Interleukin-6	**TLR**	Toll-like Receptor
IRAK4	Interleukin-1 Receptor-associated Kinase 4	**TNF-α**	Tumor Necrosis Factor α
JNK	c-Jun N-terminal Kinase		

Anti-Inflammatory Effects of Sulfatide in Macrophage through
Inhibition of HMGB1 Secretion

Hee Sue Kim

Department of Medicine or Medical Science
The Graduate School, Yonsei University

(Directed by Professor Jeon-Soo Shin)

I. INTRODUCTION

Approximately 45 years have passed since the HMGB1 protein, an abundant nuclear protein and a well-defined danger-associated molecular pattern (DAMP) molecule, was first purified [1]. Since its discovery, HMGB1 has been discussed in various contexts. Nuclear HMGB1 is well-known for its chaperone-like functions, playing a role in deoxyribonucleic acid (DNA) unwinding [2] and DNA synthesis [3] by binding to DNA in a sequence-independent manner [4] and in the structuring of chromatin [5]. In contrast, research regarding cytosolic HMGB1 is still in its relatively early stages, revealing its role in autophagy regulation [6] and unconventional protein secretion [7].

HMGB1 can be either passively released through non-apoptotic cell death, such as in necrotic cells [8], or actively secreted through multiple pathways, such as in inflammasome-mediated release [9]. In this paper, I intend to limit the scope to active secretion of HMGB1, triggered by inflammatory signals transduced by toll-like receptor (TLR)-related signaling. When TLRs are stimulated by their ligands, NF-κB [10] and MAPK [10–12] are responsible for the translocation and secretion of these receptors to the extracellular space. My research concentrates on TLR4, a member of the TLR family, which recognizes lipopolysaccharides (LPS), and its mechanism of action regarding the active secretion of HMGB1. Under physiological conditions, bacterial LPS, which normally forms a micelle, is recognized by the LPS-binding protein (LBP), which facilitates its monomerization by CD14 [13]. The LPS–LBP complex, now bound to CD14, is then transferred to the myeloid differentiation protein-2 (MD-2)–TLR4 complex [14]. This complex then forms a dimer, completing its activation process. TLR4 dimers, however, require the formation of a lipid raft, a special nano-scale membrane structure consisting of various lipids [15]. TLR4, which contains lipid-binding motifs, is attracted and can readily form a dimer within the lipid rafts, providing a platform on which the TLR4s can be within closer proximity [16]. Such receptor signaling is one of many signals known to not

only trigger HMGB1 secretion, but also induce polarization of macrophages from inert, naïve macrophage to pro-inflammatory M1 macrophage [17,18]. M1 macrophage exhibits various different phenotypes compared to its counterpart, M2 macrophage, including cytokine profiles and metabolic differences [19–21].

Most studies addressing the immunological role of HMGB1 have focused on the role of extracellular HMGB1 as a DAMP molecule and its chemokine-like behavior. Depending on its redox status, HMGB1 exerts different characteristics: 1) as a thiol isoform, in which all of the three active cysteine residues (Cys23, 45, and 106) are in free-thiol(-SH) form, HMGB1 binds to C-X-C motif ligand 12 (CXCL12) and shows chemokine-like activity, recruiting immune cells to the site of inflammation [22]; 2) the disulfide isoform of HMGB1, which possesses one intra-molecular disulfide bond between the two cysteine molecules Cys23 and Cys45, exerts cytokine-like activity, activating macrophages and lymphocytes [23–25]; 3) the oxidized isoform of HMGB1, containing fully oxidized cysteine residues (-SOOOH) is considered immunologically inert [26,27]. In sepsis, extracellular HMGB1 is known to be released in its reduced form [28]; it is considered a potent pro-inflammatory cytokine [29] and a promising therapeutic target in clinical studies [30,31].

Sulfatide, also known as 3-O-sulfogalactosylceramide, is a lipid commonly found in the myelin sheath in both the central and peripheral nervous system [32]. First isolated and partially characterized over 40 years ago [33], sulfatide was suggested to play a varying role in physiological functions, ranging from myelination of nerves [34,35] to insulin secretion [36–39]. Similar to HMGB1, intracellular (or membrane-bound) sulfatide and extracellular sulfatide play different roles. While the intracellular (or membrane-bound) form performs the abovementioned functions, extracellular sulfatide can bind to selectins to cause hemostasis [40] or metastasis of tumors [41] or bind to CD1d activating natural killer T (NKT) cells with various anti-inflammatory abilities [42–46]. Although most papers discussing the anti-inflammatory functions of sulfatide emphasize on NKT cells, a report suggested that sulfatide may have a direct effect on brain-resident immune cells, causing inflammation [47]. This discrepancy between immune cells residing in the central or peripheral nervous system led us to investigate the direct effect of sulfatide in peripheral immune cells, namely the macrophages.

In this study, I aimed to elucidate the effect of sulfatide in the context of innate immunity by investigating its effect on HMGB1 secretion under LPS stimulus and discuss the specific molecules involved in the process.

II. MATERIALS AND METHODS

1. Cell culture and treatment reagents

Raw 264.7 cells were cultured in Dulbecco's Modified Eagle's Medium supplemented with 10% heat-inactivated fetal bovine serum (Gibco, Waltham, MA, USA), 100 U/mL of penicillin, and 100 μg/mL of streptomycin (Sigma, Saint Louis, MO, USA). Treatment was performed after allowing the cells to adapt to Opti-MEM (Gibco) for 2 hrs, after which the media was replaced.

LPS (*Escherichia coli* O111:B4; > 3 x 10^6 EU/mL; Sigma), sulfatide (Bovine; brain; Matreya, State College, PA, USA), 18:0(2R-OH) sulfogalactosylceramide (synthetic; Avanti, Alabaster, AL, USA), C24:0 mono-sulfogalactosylceramide (synthetic; Avanti), C24:1 mono-sulfogalactosylceramide (synthetic; Avanti), galactosylceramide (Bovine; Matreya), and ceramide (Bovine; Matreya) were used as indicated in the figures. All experiments were performed using vehicle as a negative control.

2. Bone marrow-derived macrophage (BMDM) preparation

Wild-type C57BL/6 mice obtained from Orient Bio (Seongnam, Gyeonggi-do, South Korea) were housed in a SPF-grade facility with controlled temperature, humidity, and light. For all experiments, 8-week old female mice with approximate body weight of 20 g were used. The animals were ethically sacrificed, and the femur and tibia were extracted. Bone marrow was collected via warm, serum-free DMEM lavage until no remaining bone marrow was visible. Bone marrow was collected and filtered through cell strainer with 40 μm pore (SPL, Pocheon-si, Gyeonggi-do, South Korea) to remove any undesirable debris and washed with excessive media to further remove unfiltered debris. The resulting cells were plated to 100 mm cell culture-treated dish (Corning, Oneonta, NY, USA), and then differentiated using 20 ng/mL GM-CSF in complete medium for 7 days to yield BMDMs.

3. Sample preparation (culture media)

Culture media after treatment were collected after 24 hrs to compare HMGB1 secretion between groups. Culture media were then centrifuged at $3,500 \times g$ for 5 mins to remove any cell debris. The supernatant was collected for trichloroacetic acid (TCA)/acetone precipitation. Then, 10% by volume of ice-cold TCA was added to the samples and mixed by inverting. After incubating overnight at -20˚C, the samples were thawed and centrifuged at $20,000 \times g$ for 90 mins. Supernatants were then discarded. The remaining pellets were washed with -20˚C acetone by vortexing vigorously and left overnight at -20˚C. Samples were centrifuged at $20,000 \times g$ for 90 mins, and the

resulting supernatants were removed. The remaining pellets were then dried and boiled with 2X sample buffer.

4. Sample preparation (whole cell lysate)

Cells were harvested by scraping using cold Dulbecco's phosphate buffered saline (PBS) after the indicated time periods; they were then collected by centrifuging at 3,000 × g for 5 mins. Supernatants were discarded, and radioimmunoprecipitation (RIPA) buffer was added before sonication. Lysed cells were centrifuged at 20,000 × g for 10 mins to remove any debris. The resulting whole cell lysates were collected, and protein concentration was quantified using the bicinchoninic acid (BCA) assay. The cell lysates were then prepared by heating to 65°C for 10 mins after adding sample buffer to minimize the loss of phosphorylated protein to beta-elimination.

5. Western blot

SDS-PAGE was performed on samples prepared via the abovementioned methods, and proteins were transferred to a polyvinylidene difluoride (PVDF) membrane for western blotting. Transferred membranes were blocked using 5% skimmed milk. Primary antibodies for HMGB1 (Abcam; Cambridge, UK), JNK (phospho- and whole; Cell Signaling Technology; Danvers, MA, USA), ERK1/2 (phospho- and whole; Cell Signaling Technology), p38 (phospho- and whole; Cell Signaling Technology), phospho-IκBα (Cell Signaling Technology), phospho-IRAK4, phospho-TBK1 (Cell Signaling Technology), caveolin 1 (Merck; Darmstadt, Germany), TLR4 (Santa Cruz; Dallas, TX, USA), and β-actin (Santa Cruz) were diluted in 5% skimmed milk solution and incubated overnight at 4°C. After extensive washing, the corresponding secondary antibody solutions were incubated for 1 hr at room temperature (20 ~ 25°C). The membranes were then washed, and signals were detected using enhanced chemiluminescence substrate solution (Gendepot; Katy, TX, USA) and X-ray film (AGFA; Mortsel, Belgium). Membranes were stripped using stripping solution (BioMax, Seoul, South Korea) for re-blotting, as necessary. Densitometry analysis was performed using Image J.

6. Immunofluorescence

Raw 264.7 cells were seeded in 4-well chambered glass slides coated with poly-L-lysine (Sigma). Treatment dosage for LPS was increased to 200 ng/mL to facilitate visualization via immunofluorescence, and sulfatide dosage was adjusted accordingly to maintain molar ratio. Treatment was performed for the duration indicated in Figure Legends. After treatment, cells were then fixed with 4% paraformaldehyde overnight in 4°C. On the subsequent day, the cells were washed with PBS and permeabilized with 1% Triton X-100 and blocked with bovine serum albumin (BSA). Primary antibodies anti-p65 (Santa Cruz) or anti-HMGB1 (Abcam) were diluted in BSA solution and left to incubate

overnight at 4˚C. After thorough washing, the respective secondary antibodies conjugated with Alexa Fluor 488 (Invitrogen; Waltham, MA, USA) were diluted in BSA solution and incubated at 37˚C for 45 mins. Slides were then washed, dried, and mounted using mounting medium containing 4′,6-diamidino-2-phenylindole (DAPI; Vector). Sealed slides were observed via FV1000 confocal microscopy (Olympus). Localization of sulfatide was determined by treating Raw 264.7 cells with biotin-sulfatide and staining them with streptavidin-Alexa Fluor 488 (Invitrogen). Localization of TLR4 was detected using mouse anti-TLR4 antibodies (Invitrogen).

7. ROS detection

Raw 264.7 cells were pre-treated with either vehicle control or 20 μM of sulfatide and with vehicle control or 100 ng/mL of LPS for 1 hr. The treatment medium was removed, and culture dishes were washed twice with warm culture medium. H2-DCFDA (Thermo Fisher; Waltham, MA, USA) was treated as per the manufacturer's instructions. Cells were viewed under a fluorescence microscope. For flow cytometric analysis of ROS levels, the cells were detached before H2-DCFDA treatment.

8. Lipid raft staining

Raw 264.7 cells were seeded in 4-well chambered glass slides coated with poly-L-lysine (Sigma). Treatment dosage for LPS was increased to 1 μg/mL to maximize lipid raft formation and facilitate visualization via immunofluorescence, and sulfatide dosage was adjusted accordingly to maintain molar ratio. Treatment was performed for the duration indicated in Figure Legends. After treatment, the cells were then washed once with 4˚C complete growth medium. Washed cells were incubated in cholera toxin B-Alexa Fluor 549 (Invitrogen) staining solution, prepared in 4˚C complete growth medium. Cells were washed with ice-cold PBS three times and fixed with ice-cold 4% paraformaldehyde for 15 mins.

9. Lipid raft isolation

Raw 264.7 cells were treated with reagents for 8 mins as indicated in the legends, and cells were briefly washed three times with ice-cold PBS to halt the internalization of lipid rafts. Cells were then lysed using the ice-cold buffer provided by Caveolea/Rafts Isolation Kit (Merck) supplemented with Triton X-100. Lysates then underwent ultracentrifugation with OptiPrep^{TM} density gradient, provided by the aforementioned kit, and nine fractions were collected. Collected fractions were then supplemented with 1% SDS to assist complete dissociation of the protein from the lipids. Treated samples were concentrated using TCA/Acetone and analyzed by immunoblotting.

10. Animal experiments

Wild-type C57BL/6 mice obtained from Orient Bio (Seongnam, South Korea) were housed in a SPF-grade facility with controlled temperature, humidity, and light. For all experiments, 8-week old female mice were used. For serum collection, mice were anesthetized using an isoflurane–oxygen mixture, and combinations of PBS, LPS (3 mg/kg), or sulfatide (25 nmol) were injected with a total of 100 μL injection volume, intraperitoneally. The animals were allowed 60 min between injections to fully recover from the effects of anesthesia. Serum samples were collected after 18 hrs. Survival rate was measured by following the same procedure as mentioned above, with increased doses of LPS and sulfatide injection (to 20 mg/kg and 175 nmol, respectively). Mice were checked twice every day and observed until completion. Survival data were then analyzed through Kaplan-Meier survival analysis. Pathological scores were obtained using the scoring regimen described by Shrum *et al.* [48], and the obtained scores were then analyzed through ANOVA and Dunnett's multiple comparison test. All experiments were conducted according to procedures approved by the Institutional Animal Care and Use Committee of the Yonsei Laboratory Animal Research Center (YLARC, 2015-0275).

11. Enzyme-linked immunosorbent assay (ELISA)

Tumor necrosis factor α (TNF-α) and interleukin-6 (IL-6) ELISA were performed using Raw 264.7 cell culture medium. Cells were treated with vehicle control (negative control), 100 ng/mL LPS, and sulfatide 20 μM, followed by LPS 100 ng/mL. Culture media were collected after 12 hrs of treatment and centrifuged to remove any cell debris. ELISA was performed with the resulting supernatant following the manufacturer's instructions (Invitrogen). Serum obtained from murine experimental sepsis models was analyzed for HMGB1, TNF-α, and IL-6 levels with HMGB1 ELISA kit (IBL International), and corresponding ELISA kits following the manufacturer's instructions.

12. Metabolic assay

Raw 364.7 cells were plated to cell culture treated XF24 plate (Agilent; Santa Clara, CA, USA) and were kept at normal mammalian cell culture condition overnight. Original culture media was changed with fresh culture media, and cells received 1 μg/mL of LPS 2 hrs prior to receiving 200 μM of sulfatide. Cells were then treated for 2 hrs and the treatment media was substituted with DMEM free of sodium bicarbonate, sodium pyruvate, and HEPES. After 30 mins of adaptation period, XF24 plate was analyzed through Seahorse XF24 Analyzer (Agilent) for extracellular acidification rate (ECAR) and oxygen consumption rate (OCR). Mitochondrial stress test was performed using Seahorse XF Cell Mito Stress Test Kit (Agilent), as per instruction supplied by the manufacturer.

13. Statistical analysis

Unless specified otherwise, statistical analysis of experimental data present in this paper were performed with Student's t test and ANOVA, with Tukey's multiple comparison test as post-hoc test, using GraphPad Prism 5. The data represent the mean value and SD. The difference was considered statistically significant at $p < 0.05$.

III. RESULTS

1. Sulfatide inhibits HMGB1 and pro-inflammatory cytokines release

To study whether sulfatide treatment shows pro-inflammatory or anti-inflammatory characteristics, I analyzed the secretion level of a well-known DAMP molecule, HMGB1. When treated simultaneously, sulfatide exhibited an inhibitory effect in HMGB1 secretion without toxicity in a dose-dependent manner, as shown (Figure 1A). This phenotype was unique to sulfatide, and was not seen in its precursors, galactosylceramide and ceramide (Figure 1B). Further analysis using ligands of other extracellular TLRs or other PTM provoking stimuli show complete inhibition of HMGB1 secretion (Figure 1C). This indirectly suggests that the anti-inflammatory effect does not come from inhibiting the ligand-receptor interaction by acting as a competitive inhibitor or aggregating reagent against TLR ligands, since it is unlikely that a molecule can act as broad-range inhibitor or aggregating reagent against multiple TLR ligands with different characteristics.

Next, the time point-dependent effect of sulfatide was studied to further investigate the mechanism of action (Figure 1D). Interestingly, sulfatide not only exhibited dose- and time-dependent manner in HMGB1 release suppression, but also removal of sulfatide only induced a slight increase – lower than the secretion level of negative control, nevertheless – in HMGB1 secretion in 6 and 12 hr-pretreatment samples. Same phenomenon was also observed in post-treatment samples, showing inhibitory effect up to 6 hrs of post-treatment. These results, combined with the results collected above, suggest that sulfatide is neither an aggregating reagent nor competitive inhibitor, nor a reversible non-competitive inhibitor of TLR ligands.

Although multiple points of inhibition are potentially available throughout the HMGB1 secretion pathway, they can be categorized into two large categories: initial signal transduction, and the release step. In order to clarify whether sulfatide affects the former or the latter, I treated Raw 264.7 cells with LPS or sulfatide and investigated HMGB1 localization via immunofluorescence microscopy (Figure 1E). Confocal microscopy images show sulfatide inhibits nuclear HMGB1 translocation to the cytoplasm caused by LPS stimulation. This indicates that the inhibition mechanism of sulfatide does not target the release of HMGB1 to the extracellular space itself, but the pathway that precedes HMGB1 translocation.

A

| LPS | - | + | - | - | + | + | (100 ng/mL) |
| Sulfatide | - | - | 2 | 20 | 2 | 20 | (µM) |

HMGB1
Ponceau S

| LPS | - | + | + | + | + | + | + | + | + | + | (100 ng/mL) |
| Sulfatide | - | - | 0.1 | 0.5 | 1 | 2 | 5 | 10 | 15 | 20 | (µM) |

HMGB1
Ponceau

B

| LPS | - | + | - | - | + | + | (100 ng/mL) |
| Cer | - | - | 2 | 20 | 2 | 20 | (µM) |

HMGB1
Ponceau

| LPS | - | + | - | - | + | + | (100 ng/mL) |
| GalCer | - | - | 2 | 20 | 2 | 20 | (µM) |

HMGB1
Ponceau

C

| LTA | - | + | + | (10 µg/mL) |
| Sulfatide | - | - | + | (20 µM) |

HMGB1
Ponceau S

| Flagelin | - | + | + | (1 µg/mL) |
| Sulfatide | - | - | + | (20 µM) |

HMGB1
Ponceau S

LPS	-	100	100	-	-	-	-	-	-	-	-	-	(ng/mL)
H₂O₂	-	-	-	-	0.1	0.1	-	-	-	-	-	-	(mM)
TSA	-	-	-	-	-	-	10	10	-	-	-	-	(ng/mL)
PMA	-	-	-	-	-	-	-	-	-	100	100	-	(nM)
Sulfatide	-	-	20	-	-	20	-	20	-	-	20	-	(uM)

HMGB1
Ponceau

D

Unwashed

		Pre-treatment time (h)				Post-treatment time (h)				
LPS	-	+	+	+	+	+	+	+	+	+	(100 ng/mL)
Sulfatide	-	-	12	6	2	1	1	2	6	12	(20 µM)

HMGB1 (S.E)
HMGB1 (L.E)
Ponceau S

Washed

		Pre-treatment time (h)				Post-treatment time (h)				
LPS	-	+	+	+	+	+	+	+	+	+	(100 ng/mL)
Sulfatide	-	-	12	6	2	1	1	2	6	12	(20 µM)

HMGB1 (S.E)
HMGB1 (L.E)
Ponceau S

E

DAPI   HMGB1   Merge

Control

LPS

Sulfatide

Sulfatide
LPS

10µm

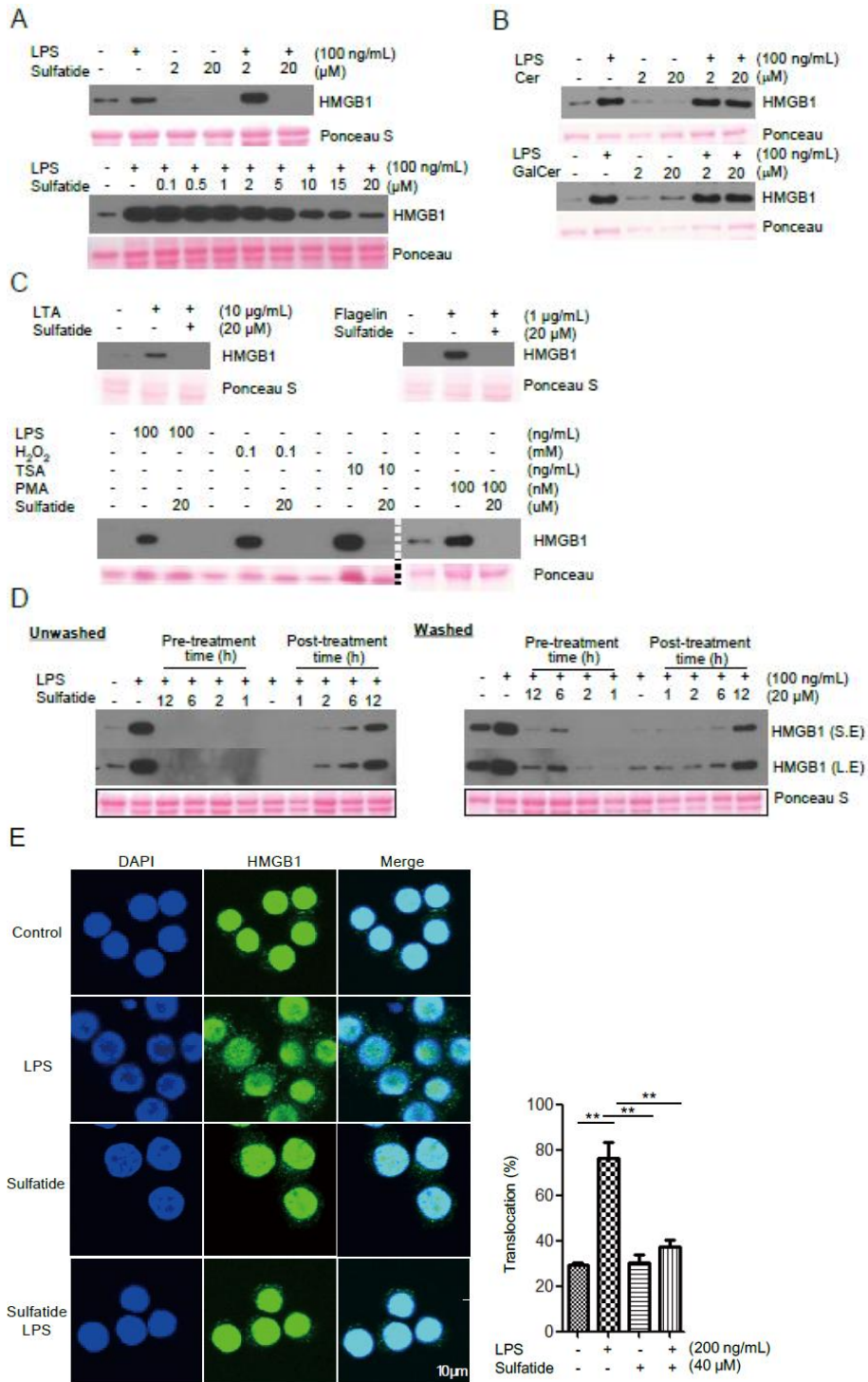| LPS | - | + | - | + | (200 ng/mL) |
| Sulfatide | - | - | + | + | (40 µM) |

Translocation (%)

– 12 –

Figure 1. Sulfatide inhibits HMGB1 translocation and release in Raw 264.7 cells. (A) Dose-dependency and toxicity test of sulfatide regarding HMGB1 secretion was accessed 24 hrs after LPS treatment. Varying dosage of sulfatide was treated 10 mins prior to LPS treatment. Resulting culture media were concentrated using TCA/Acetone precipitation as described in the Methods section and were immunoblotted. (B) Treatment with galactosylceramide or ceramide was done before LPS or vehicle controls were applied to Raw 264.7 cells. Cells received the abovementioned stimuli and were cultured for 24 hrs. Culture media were concentrated and analyzed by immunoblotting as described in the Methods section. (C) Raw 264.7 cells were treated with other extracellular TLR ligands and PTM-inducing stimuli after sulfatide treatment. Culture media were concentrated and analyzed by immunoblotting as described in the Methods section. (D) Efficacy of sulfatide pre-treatment for indicated time on HMGB1 secretion and its effect after removal of sulfatide was observed. Washed cells received two 36°C PBS wash to remove the residual sulfatide prior to LPS treatment, whereas unwashed cells were left unperturbed. (SE = Short Exposure, LE = Long Exposure) (E) Raw 264.7 cells received vehicle control, LPS 200 ng/mL, sulfatide 40 μM only, or 10 mins of sulfatide 40 μM pre-treatment, followed by LPS 200 ng/mL for 6 hrs. Cells were fixed for analysis by immunofluorescence, as described in the Methods section. In total, 100 cells were counted, and those containing HMGB1 signals in the cytoplasm were counted as positive. Statistical analysis was performed by analyzing data from 3 independent trials. $*p < 0.01$, $**p < 0.001$.

2. Sulfatide down-regulates NF-κB signaling pathway and JNK phosphorylation

The pathway most frequently associated with TLR signaling, NF-κB signaling pathway, is a cascade of signaling molecules that results in the degradation of NF-κB inhibitory molecules and the translocation of NF-κB to the nucleus, acting as a transcription factor. Concerning this pathway, I performed immunofluorescence microscopy, tracking the location of the p65 molecule, and immunoblotting of the IκBα molecule (Figure 2A, 2B). Our immunofluorescence data shows that NF-κB activation, signified by the translocation of p65, decreased when cells were pre-treated with sulfatide. Immunoblotting also indicated that phosphorylation of IκBα, a crucial step that precedes its ubiquitination and degradation, significantly decreases when pre-treated with sulfatide.

Further analysis of the MAPKs within the TLR signaling pathway revealed specific kinases affected by sulfatide treatment. The phosphorylation levels of ERK, JNK, and p38 MAPK were analyzed via immunoblotting (Figure 2C). Immunoblots revealed that only the phosphorylation level of JNK, but not of ERK or p38, was decreased by pre-treatment with sulfatide. Overall, sulfatide blocks the NF-κB signaling pathway and JNK-mediated HMGB1 translocation.

Previous reports state sulfatide to play a pro-inflammatory role in brain-resident immune cells [47]. In order to confirm its anti-inflammatory characteristics shown within my experimental setup, I treated Raw 264.7 cells with vehicle control, LPS alone, or LPS stimuli after sulfatide pre-treatment (Figure 2D). Contrary to previous reports made with brain-resident immune cells, sulfatide did not induce any significant secretion of pro-inflammatory cytokines, namely TNF-α and IL-6. Interestingly, a combination of LPS and sulfatide, however, did result in a significant decrease in the secretion levels of both TNF-α and IL-6, indicating that sulfatide indeed has an anti-inflammatory role in the peripheral immune system.
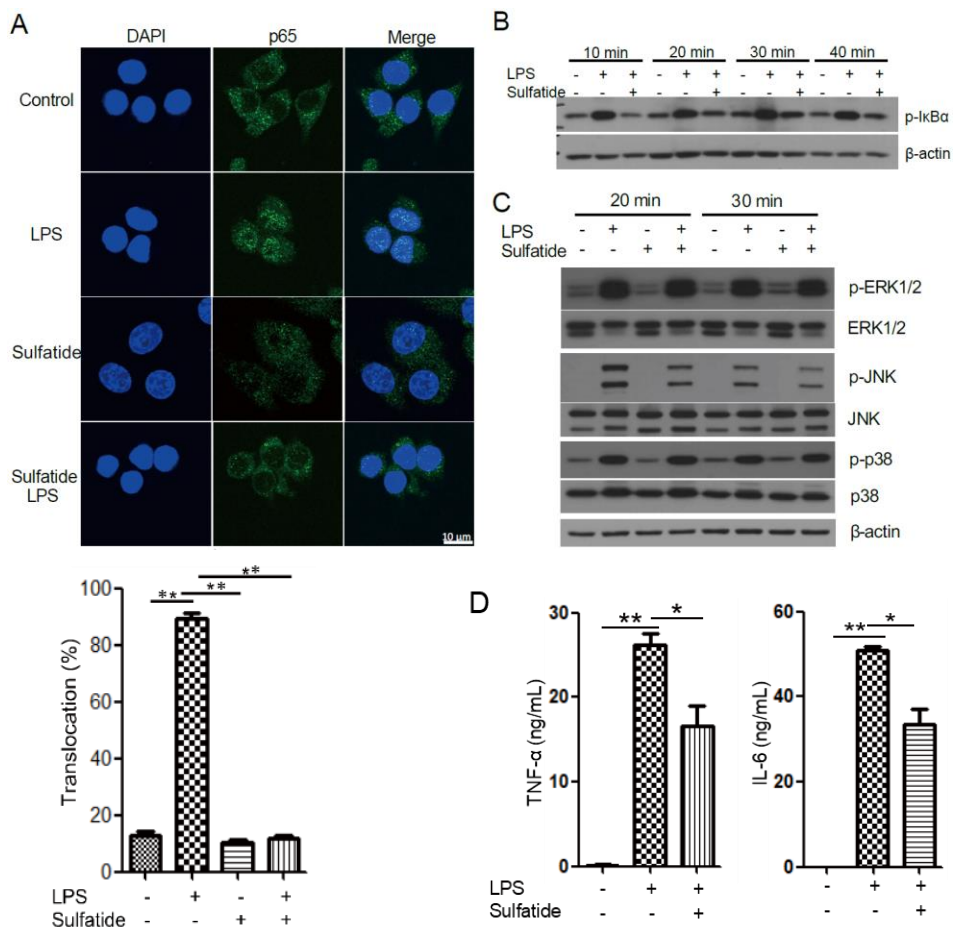
Figure 2. Sulfatide suppresses NF-κB activation and JNK phosphorylation.
(A) Raw 264.7 cells received vehicle control, LPS 200 ng/mL, sulfatide 40 μM, or 10 mins of 40 μM sulfatide pre-treatment, followed by LPS 200 ng/mL for 40 min. Cells were then fixed for analysis by immunofluorescence as described in the Methods section. In total, 100 cells were counted, and those with p65 signals co-localizing with DAPI were counted as positive. * $p < 0.001$. (B, C) Raw 264.7 cells received vehicle control, LPS 100 ng/mL, sulfatide 20 μM, or 10 mins of 20 μM sulfatide pre-treatment followed by LPS stimuli, as shown in the figure. Cells were harvested after the indicated times and analyzed for the phosphorylation level of IκBα (B), p-ERK, p-JNK, and p-p38 (C) by immunoblotting. (D) Culture media were analyzed by ELISA for TNF-α and IL-6 titer. Cells were treated with vehicle control (PBS with DMSO), LPS 100 ng/mL, or 10 mins of sulfatide 20 μM pre-treatment, followed by LPS 100 ng/mL. All graphs show the mean value and error bars of three independent experiments performed. * $p < 0.01$, ** $p < 0.001$.

– 15 –

3. LPS-mediated ROS production is decreased by sulfatide

Since an alternate mechanism exists, where HMGB1 release can be triggered via LPS-TLR4 signaling through ROS production, I sought to measure the changes in the level of intracellular ROS in the presence/absence of sulfatide pre-treatment (Figure 3A, 3B). Flow cytometric analysis and measurement of relative fluorescence intensity both show a significant decrease in intracellular ROS levels in sulfatide pre-treated groups. Such a decrease in ROS levels can be accredited to the decreased phosphorylation of both TBK1 and IRAK4, molecules that play crucial roles in the regulation of NOX activity (Figure 3C). These results, paired with those presented in earlier experiments, propose that the point of inhibition, which sulfatide utilizes to suppress HMGB1 release is positioned higher in the signaling hierarchy.
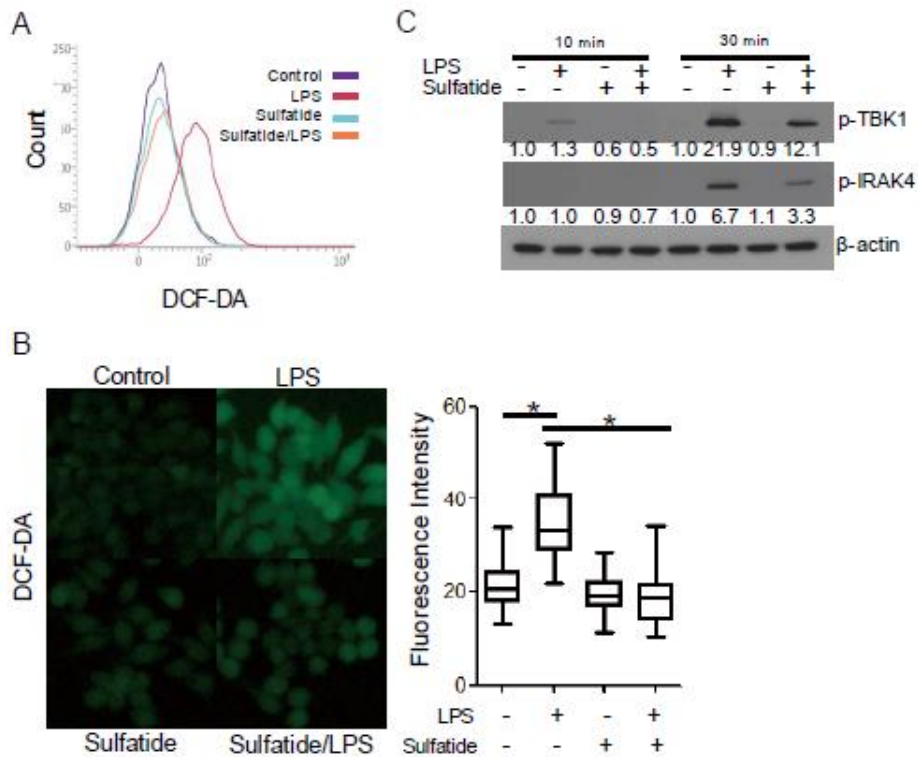
Figure 3. Sulfatide down-regulates LPS-induced ROS production. Raw 264.7 cells were treated with 20 μM sulfatide or vehicle control for 10 mins prior to receiving LPS 100 ng/mL, and were treated with DCF-DA. Resulting cells were analyzed through (A) flow cytometry and (B) fluorescence microscopy. More than 150 cells were counted. Statistical analysis was performed based on data from 3 independent trials. * $p < 0.001$. (C) Cells were pre-treated with vehicle control or 20 μM sulfatide before treatment with 100 ng/mL LPS. Cells were lysed, and the samples were immunoblotted for p-TBK1 and p-IRAK4. Numbers below the immunoblots represent the relative band intensity, obtained by densitometry analysis. Vehicle controls of each groups were considered as standards.

4. Sulfatide hinders the translocation of TLR4 into lipid rafts

I hypothesized that sulfatide, a well-known component of the cell membrane, may interfere with the lipid composition of the cell membrane, inhibiting its signaling pathways. Since TLR4 requires its monomers to be localized within the lipid raft microdomains to form dimers, I sought to assess 1) whether sulfatide localizes to the lipid raft microdomains, and 2) whether sulfatide treatment curbs the localization of TLR4 to lipid rafts. Utilization of biotinylated sulfatide revealed the co-localization of sulfatide and lipid rafts (Figure 4A), indicating the possibility of direct involvement of sulfatide in the lipid raft machinery. Next, to observe the co-localization of TLR4 and lipid rafts, I treated cells with appropriate stimuli and were prepared for immunofluorescence. Results insinuated that sulfatide plays a role in significantly decreasing the localization of TLR4 into the lipid microdomains. Such findings were reinforced by subjecting the cells to identical conditions and fractionating the cell lysate for lipid rafts. Results showed significantly decreased co-localization of TLR4 within the lipid raft fractions, signified by caveolin-1, in sulfatide-treated groups. In summary, sulfatide was found to interfere with the localization of TLR4 within lipid rafts, decreasing the efficacy of TLR4 signaling (Figure 4B, 4C).
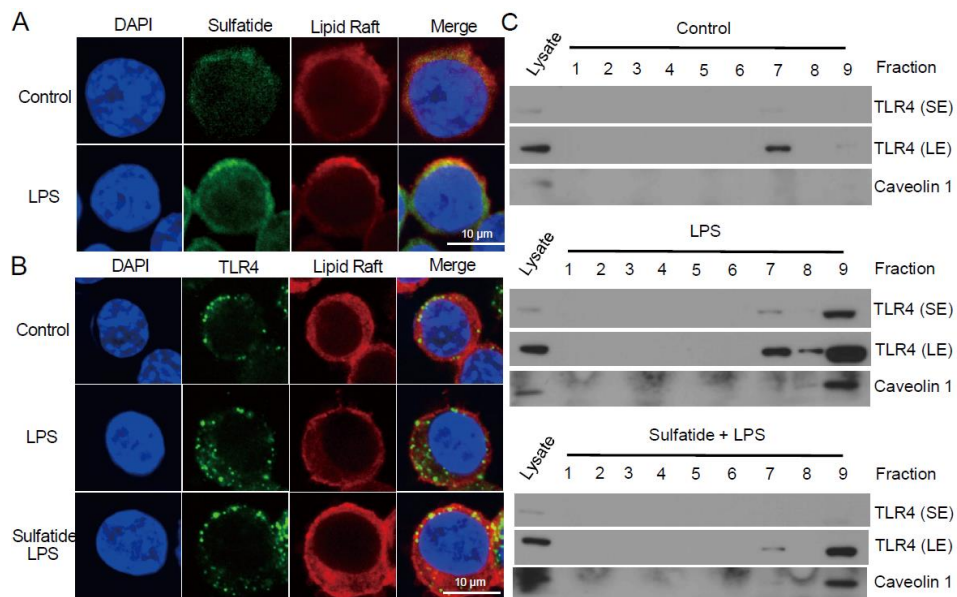
Figure 4. TLR4–lipid raft complex formation is reduced by sulfatide. (A) Raw264.7 cells were treated with 200 μM of biotinylated sulfatide, with or without 1 μg/mL of LPS for 8 mins. Biotinylated sulfatide was stained with streptavidin-Alexa Fluor 488 and lipid raft with cholera toxin B-Alexa Fluor 549, and the cells were prepared for confocal microscopy as described in the Methods section. (Scale bar : 10 μm) (B) Raw 264.7 cells were treated with vehicle control or 40 μM of sulfatide for 10 mins, before 8 mins of vehicle control or 200 ng/mL of LPS treatment. TLR4 was stained with anti-TLR4 antibody and anti-rabbit IgG-Alexa Fluor 488 and lipid raft with cholera toxin B-Alexa Fluor 549, and the cells were prepared for confocal microscopy as described in the Methods section. (Scale bar : 10 μm)   (C) Raw 264.7 cells were identically treated as those in Figure 4B, and obtained samples were immunoblotted for TLR4 and caveolin 1. All membranes were immunoblotted under identical medical X-ray film for accurate comparison. (SE = Short Exposure, LE = Long Exposure)

5. Release of HMGB1 is suppressed by sulfatide in BMDM and the murine experimental sepsis model

The effects of sulfatide in primary cells and *in vivo* murine models were measured. BMDMs of 8 weeks old female C57BL/6 mice were harvested and were subjected to the same stimuli used above (Figure 5A). BMDMs pre-treated with sulfatide showed significantly decreased HMGB1 secretion, compared to cells treated with LPS alone, congruent with data obtained with Raw 263.7 cells. Such conformity led us to induce an experimental septic shock by the means of a sub-lethal dose injection of LPS into the peritoneum of C57BL/6 mice. Measurement of serum HMGB1 level was taken from sera obtained from a total of 18 mice (Figure 5B). Serum HMGB1 level was significantly decreased in the groups pre-treated with sulfatide, compared to groups treated only with LPS (Figure 5B). These results show that sulfatide regulates the release of HMGB1, a late time point cytokine of sepsis, in the murine experimental sepsis model. Such decrease in the serum HMGB1 level is also reflected in the murine model injected with a lethal dosage of LPS, mimicking acute septic shock. Although showing the telltale signs of septic shock (decreased physical activity, shivering etc.), mice pre-injected with sulfatide before LPS injection experienced no death in the population, in contrary to those that received saline pre-injection (Figure 5C). Additionally, to accurately compare the severity of the septic shock and the effect of sulfatide in decreasing its severity, pathological scores were measured every 24 hrs. Sulfatide pre-injected mice showed similar increase in pathological scores as the mice injected only with LPS for the first 24 hrs; however, groups that only received LPS injection showed a continuous increase in pathological scores, whereas the scores of the sulfatide pre-injected group plateaued, followed by a decrease in the pathological score (Figure 5D). Generally, sulfatide successfully blocked the LPS-mediated HMGB1 release in sepsis, decreasing the level of serum HMGB1 and preventing severe symptoms and death caused by sepsis.
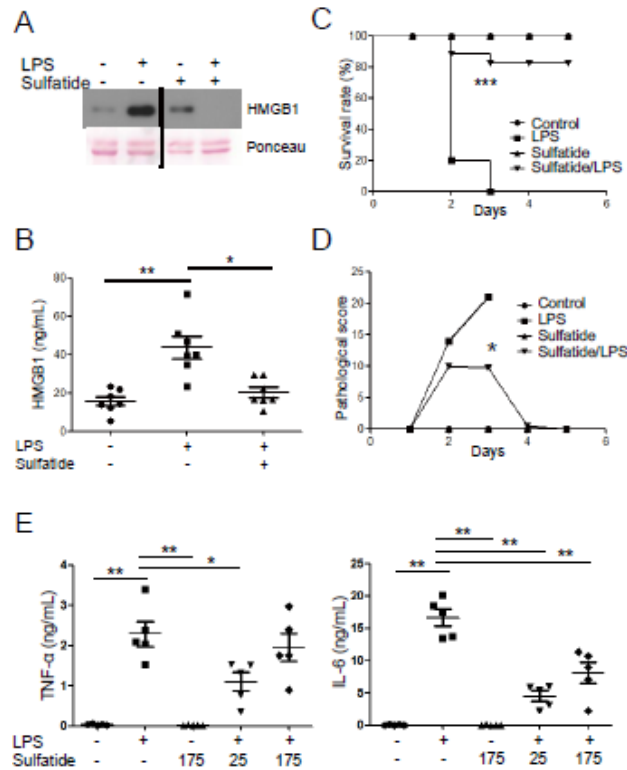
Figure 5. Sulfatide decreases HMGB1 release in mouse BMDMs and the murine experimental sepsis model. (A) BMDMs were subjected to vehicle control, LPS 100 ng/mL, and 10 mins of 20 μM sulfatide pre-treatment, followed by LPS 100 ng/mL for 24 hrs. The dotted line indicates where different portion of the identical membrane have been presented together. (B) C57BL/6 mice (7 mice per group) were intraperitoneally injected with PBS, 3 mg/kg of LPS, or 25 nmol sulfatide pre-treatment, followed by LPS injection, as discussed in the Methods section. Sera were harvested and prepared for ELISA to measure serum HMGB1 level. (C) C57BL/6 mice (5 mice per group) were subjected to a survival test against LPS-induced lethal septic shock of 20 mg/kg of LPS injection. Two independent trials were completed, and the results were pooled for statistical analysis via Kaplan-Meier survival analysis. (D) A pathological score was obtained from the mice described in Figure 5C. Mice from the second trial were used. (E) C57BL/6 mice (5 mice per group) were intraperitoneally injected with PBS or sulfatide pre-treatment (25 or 175 nmol), followed by LPS injection of 3 mg/kg, as described in the Methods section. Sera were harvested and prepared for ELISA to measure serum TNF-α and IL-6 level. $*p < 0.01$, $**p < 0.001$, $***p < 0.0001$.

6. Sulfatide exert anti-inflammatory potential through shifting metabolic characteristics

Aforementioned anti-inflammatory potential of sulfatide spanned from 12 hrs pre-treatment to 6 hrs post-treatment in regards of inhibiting HMGB1 secretion (Figure 1D). Since sulfatide hindering TLR4 – lipid raft colocalization is thought to be the mechanism behind the anti-inflammatory phenotype during pre-treatment, further observation was performed to study the mechanism responsible for post-treatment. Raw 264.7 cells were treated with LPS prior to receiving sulfatide treatment and metabolic assays were carried out. LPS treatment increased ECAR, as expected from TLR4 – induced macrophage activation. Interestingly, however, sulfatide post-treatment decreases ECAR of LPS stimulated macrophages to control level (Figure 6A). Further analysis of the cells those received sulfatide after LPS treatment compared to those did not, showed difference in mitochondrial maximal respiration, indicating significant change in metabolic characteristics (Figure 6B). Post-injection of sulfatide in LPS injected mice also showed significant decrease in pro-inflammatory cytokines, such as TNF-α and IL-6 (Figure 6C).
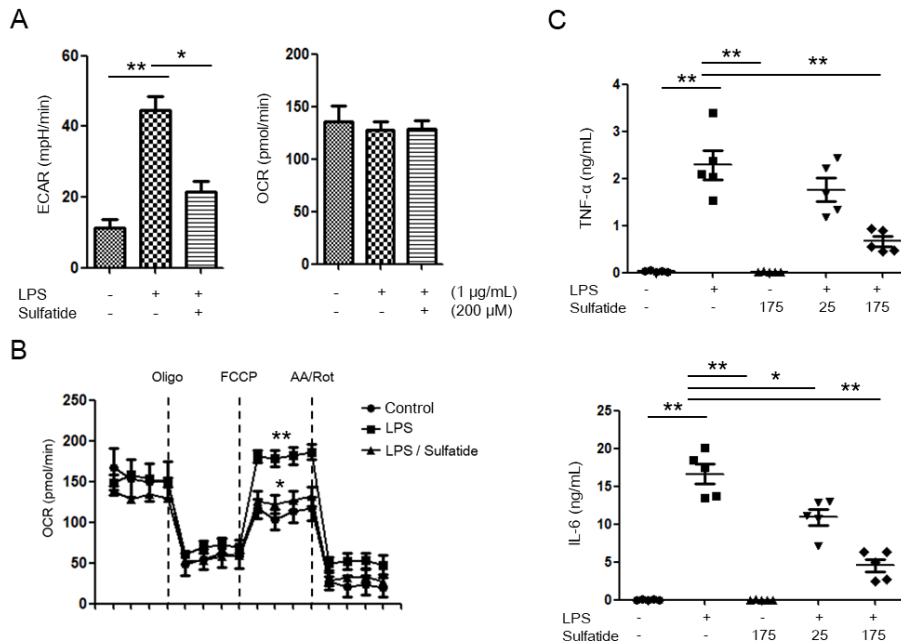
Figure 6. Sulfatide shifts metabolic characteristics, resulting in anti-inflammatory phenotype. (A) Raw 264.7 cells were analyzed with Seahorse XF24 Analyzer as described in the Methods section. Cells received 2 hrs of LPS treatment prior to 2 hrs of sulfatide treatment. Statistical analysis was performed for 4 separate data for each group. (B) Raw 264.7 cells received 2 hrs of LPS treatment prior to 2 hrs of sulfatide treatment, and were analyzed with Seahorse XF24 Analyzer for mitochondrial respiration. Oligomycin (Oligo), FCCP, and Antimycin A/Rotenone (AA/Rot) were injected to the wells at appropriate time points. Statistical analysis was performed for 3 separate data. (Control vs. LPS $p < 0.001$; LPS vs. LPS/Sulfatide $p < 0.01$) (C) C57BL/6 mice (5 mice per group) were intraperitoneally injected with 3 mg/kg of LPS, followed by PBS or sulfatide post-treatment of 25 or 175 nmol, as described in the Methods section. Sera were harvested and prepared for ELISA to measure serum TNF-α and IL-6 level. * $p < 0.01$, ** $p < 0.001$.

IV. DISCUSSION

My experiments showed sulfatide reducing HMGB1 secretion and cytosolic translocation upon LPS stimulation. Sulfatide decreased the activation of NF-κB translocation into the nucleus, and inhibition of multiple kinases, such as JNK, IRAK4, and TBK1, was also seen throughout the experiment. JNK is a well-known signaling molecule playing a crucial role in cellular stress conditions, and when activated, phosphorylated JNK can also alter the mitochondria to increase its ROS production significantly, creating a positive feedback loop [49]. Mice expressing inactive mutant form of IRAK4 were found to be more susceptible to *Listeria monocytogenes* and *Mycobacterium smegmatis* systemic infections due to impaired induction of inducible nitric oxide synthase (iNOS) mRNA [50]. Since TBK1 was also involved in mitophagic regulation of mitochondrial physiology and expression of iNOS mRNA during inflammatory assault, paired with the reduction of ROS production, I hypothesized that the inhibitory characteristics of sulfatide may come from the upper hierarchy [51,52]. Further experiments showed pre-treatment of sulfatide was hindering the lipid raft–TLR4 interaction, thereby diminishing the TLR4 signaling pathway; on the other hand, post-treatment of sulfatide showed decreasing ECAR spike caused by LPS stimulation and causing polarizing histone acetylation pattern, compared to cells those only received LPS stimulation.

Based on my research, the possibility of exogenous sulfatide as regulator of lipid raft – receptor complex formation may be suggested in clinical scenarios, in addition to the experimental sepsis model provided within. Pathological action of angiotensin II, a potent vasoconstrictor which binds to the AT_1 receptor, are ascribed to multiple vascular diseases, such as hypertension and secondary cardiac hypertrophy [53]. AT_1 receptors are reported to be associated with lipid rafts [54]; thus, sulfatide can be used to alter the lipid composition of the microdomains to deter the pathology in angiotensin II-mediated hypertension patients. Moreover, the immunological synapse, crucial for B/T cell activation, also depends on lipid raft formation [55–58], proposing a potential treatment strategy against autoimmune diseases such as rheumatoid arthritis, Type I diabetes, and multiple sclerosis [59–61] by blocking abnormal B/T cell activation.

Sulfatide, however, has been reported as a possible auto-antigen in multiple sclerosis and experimental autoimmune encephalomyelitis (EAE). Lipid microarrays showed specific antibodies against various lipids in the cerebrospinal fluid, including ones against sulfatide in the murine EAE model and in multiple sclerosis [62,63]. Kanter *et al.* also reported the increase in disease severity as the mice were immunized with sulfatide and myelin membrane

proteins. A further role of sulfatide as a pro-inflammatory molecule in pathogenesis was discovered in autoimmune hepatitis [64]. In contrast, the anti-inflammatory roles of sulfatide were also revealed in autoimmune neuritis and asthma, mediated by sulfatide-activated type II NKT cells [42,65]. These reports suggest that sulfatide can be a double-edged sword, depending on the organ and pathological context, and that caution must be taken when attempting to adapt the "natural" form of sulfatide as a potential therapeutic agent. Further studies regarding the mechanism of action of sulfatide in the abovementioned pathologies should be pursued to minimize or ameliorate side effects, possibly by utilizing small molecules mimicking the action of sulfatide.

My research was able to report the anti-inflammatory effect of sulfatide in the periphery, specify the kinases within the NF-κB and MAPK pathway affected by sulfatide, and elucidate its mechanism of action. Sulfatide, nevertheless, is naturally a mixture of varying lengths of carbon chain backbone; therefore, the sulfatide used in this experiment is close to its natural form but far from being homogenous. Such properties could control the accessibility of sulfatide isoforms to various molecules via steric hindrance and variation in affinity. The composition of sulfatide isoforms has been connected to MS prognosis, enabling physicians to differentiate remitting MS from progressive MS by studying the composition of sulfatide isoforms [66]. Although I was able to discover sulfatide hampering the localization of TLR4 and lipid rafts in my research, the specific roles of each component of sulfatide are yet to be discovered. According to the composition sheet provided by the supplier, C24-related isoforms were dominant in the making of sulfatide. This may explain the difference in phenotype between my experiment and others, as I carefully suggest the difference stems from the variability of sulfatide composition, depending on the provider. Isaac *et al.* has reported the importance of C18 sulfatide in astrocyte functionality [67], whereas many researchers including Buschard *et al.* and Blomqvist *et al.* have reported the crucial role of the C16:0 isoform in diabetes mellitus [68,69]. Such reports describing distinct role of various sulfatide components could be used to aid in indirectly understanding the phenotype difference between our group and the others. I sought to specify the isoform solely responsible for the phenotype shown within C24-related isoforms and C18 sulfatide, but to no avail (data not shown). Although I was not able to establish the isoform of sulfatide that is responsible for its properties, I was able to suggest that the mixture of C24-related isoforms and the C18 isoform that mimics the natural composition of sulfatide could also mimic its suppressive phenotype (data not shown). Fine-tuning the composition of specific isoforms by the means of supplementing the patients with sulfatide isoforms as needed may prove to be useful to alter the overall phenotype of sulfatide, further opening its therapeutic potential.

V. CONCLUSION

In conclusion, my study showed the effect of sulfatide in suppressing the secretion of HMGB1 under LPS stimulation, and its potential as anti-sepsis treatment. I have also firstly described the mechanism of inhibition where sulfatide inhibits the localization of TLR4 within the lipid microdomains, nullifying LPS-TLR4 signaling cascade, and reported metabolic and possibility of transcriptional regulation. Further investigations regarding the interaction of exogenous sulfatide with lipid microdomains, importance of sulfatide isoform composition in various inflammatory diseases, in-depth studying of isoform lipid biology, and extensive studies regarding the mechanism behind transcriptional and metabolic regulation are necessary to pursue future therapeutic applications of sulfatide.

REFERENCES

1. Goodwin GH, Sanders C, Johns EW. A new group of chromatin-associated proteins with a high content of acidic and basic amino acids. Eur J Biochem 1973;38:14–9.
2. Yoshida M, Makiguchi K, Chida Y, Shimura K. Unwinding of DNA by nonhistone protein HMG1 and HMG2. Nucleic Acids Symp Ser 1984:181–4.
3. C. B, F. H, E. P, M. D, M. RA. Nuclear accumulation of HMG1 protein is correlated to DNA synthesis. Biol Cell 1986;58:185–94.
4. YU SS, LI HJ, GOODWIN GH, JOHNS EW. Interaction of Non-histone Chromosomal Proteins HMG1 and HMG2 with DNA. Eur J Biochem 1977;78:497–502.
5. Yu S, Spring TG. The Interaction of Nonhistone Chromosomal Proteins HMG1 and HMG2 with Subfractions of H1 Histone Immobilized on Agarose. Biochim Biophys Acta 1977;492:20–8.
6. Tang D, Kang R, Livesey KM, Cheh C-W, Farkas A, Loughran P, et al. Endogenous HMGB1 regulates autophagy. J Cell Biol 2010;190:881–92.
7. Lee H, Shin N, Song M, Kang U-B, Yeom J, Lee C, et al. Analysis of Nuclear High Mobility Group Box 1 (HMGB1)-Binding Proteins in Colon Cancer Cells: Clustering with Proteins Involved in Secretion and Extranuclear Function. J Proteome Res 2010;9:4661–70.
8. Scaffidi P, Misteli T, Bianchi ME. Release of chromatin protein HMGB1 by necrotic cells triggers inflammation. Nature 2002;418:191–5.
9. Vande Walle L, Kanneganti T-D, Lamkanfi M. HMGB1 release by inflammasomes. Virulence 2011;2:162–5.
10. Wu C-X, Sun H, Liu Q, Guo H, Gong J-P. LPS induces HMGB1 relocation and release by activating the NF-kappaB-CBP signal transduction pathway in the murine macrophage-like cell line RAW264.7. J Surg Res 2012;175:88–100.
11. Jiang W, Pisetsky DS. The role of IFN-alpha and nitric oxide in the release of HMGB1 by RAW 264.7 cells stimulated with polyinosinic-polycytidylic acid or lipopolysaccharide. J Immunol 2006;177:3337–43.
12. Yang Z, Li L, Chen L, Yuan W, Dong L, Zhang Y, et al. PARP-1 Mediates LPS-Induced HMGB1 Release by Macrophages through Regulation of HMGB1 Acetylation. J Immunol 2014;193:6114 LP – 6123.
13. Yu B, Wright SD. Catalytic properties of lipopolysaccharide (LPS) binding protein: Transfer of LPS to soluble CD14. J Biol Chem 1996;271:4100–5.
14. da Silva Correia J, Soldau K, Christen U, Tobias PS, Ulevitch RJ.

Lipopolysaccharide is in close proximity to each of the proteins in its membrane   receptor complex. transfer from CD14 to TLR4 and MD-2. J Biol Chem 2001;276:21129–35.

15. Lingwood D, Simons K. Lipid rafts as a membrane-organizing principle. Science 2010;327:46–50.

16. Ruysschaert JM, Lonez C. Role of lipid microdomains in TLR-mediated signalling. Biochim Biophys Acta - Biomembr 2015;1848:1860–7.

17. Lolmede K, Campana L, Vezzoli M, Bosurgi L, Tonlorenzi R, Clementi E, et al. Inflammatory and alternatively activated human macrophages attract vessel-associated stem cells, relying on separate HMGB1- and MMP-9-dependent pathways. J Leukoc Biol 2009;85:779–87.

18. Wang N, Liang H, Zen K. Molecular Mechanisms That Influence the Macrophage M1/M2 Polarization Balance. Front Immunol 2014;5:1–9.

19. Oishi Y, Spann NJ, Link VM, Muse ED, Strid T, Edillor C, et al. SREBP1 Contributes to Resolution of Pro-inflammatory TLR4 Signaling by Reprogramming Fatty Acid Metabolism. Cell Metab 2017;25:412–27.

20. Liu PS, Wang H, Li X, Chao T, Teav T, Christen S, et al. A-Ketoglutarate Orchestrates Macrophage Activation Through Metabolic and Epigenetic Reprogramming. Nat Immunol 2017;18:985–94.

21. Rostam HM, Reynolds PM, Alexander MR, Gadegaard N, Ghaemmaghami AM. Image based Machine Learning for identification of macrophage subsets. Sci Rep 2017;7:1–11.

22. Antoine DJ, Harris HE, Andersson U, Tracey KJ, Bianchi ME. A systematic nomenclature for the redox states of high mobility group box (HMGB)   proteins. Mol Med 2014;20:135–7.

23. Yang H, Wang H, Ju Z, Ragab AA, Lundbäck P, Long W, et al. MD-2 is required for disulfide HMGB1–dependent TLR4 signaling. J Exp Med 2015;212:5 LP – 14.

24. Yang H, Antoine DJ, Andersson U, Tracey KJ. The many faces of HMGB1: molecular structure-functional activity in inflammation, apoptosis, and chemotaxis. Journal of Leukocyte Biology. Bethesda, MD, USA; 2013.

25. Gunasekaran MK, Viranaicken W, Girard AC, Festy F, Cesari M, Roche R, et al. Inflammation triggers high mobility group box 1 (HMGB1) secretion in adipose tissue, a potential link to obesity. Cytokine 2013;64:103–11.

26. Urbonaviciute V, Meister S, Furnrohr BG, Frey B, Guckel E, Schett G, et al. Oxidation of the alarmin high-mobility group box 1 protein (HMGB1) during apoptosis. Autoimmunity 2009;42:305–7.

27. Liu A, Fang H, Dirsch O, Jin H, Dahmen U. Oxidation of hmgb1 causes attenuation of its pro-inflammatory activity and occurs during liver

ischemia and reperfusion. PLoS One 2012;7.

28. Abdulmahdi W, Patel D, Rabadi MM, Azar T, Jules E, Lipphardt M, et al. HMGB1 redox during sepsis. Redox Biol 2017;13:600–7.

29. Huang W, Tang Y, Li L. HMGB1, a potent proinflammatory cytokine in sepsis. Cytokine 2010;51:119–26.

30. Wang H, Ward MF, Sama AE. Targeting HMGB1 in the treatment of sepsis. Expert Opin Ther Targets 2014;18:257–68.

31. Stevens NE, Chapman MJ, Fraser CK, Kuchel TR, Hayball JD, Diener KR. Therapeutic targeting of HMGB1 during experimental sepsis modulates the inflammatory cytokine profile to one associated with improved clinical outcomes. Sci Rep 2017;7:5850.

32. Eckhardt M. The role and metabolism of sulfatide in the nervous system. Mol Neurobiol 2008;37:93–103.

33. Levine M, Kornblatt MJ, Murray RK. Isolation and partial characterization of a sulfogalactoglycerolipid from rat brain. Can J Biochem 1975;53:679–89.

34. Ranscht B, Clapshaw PA, Price J, Noble M, Seifert W. Development of oligodendrocytes and Schwann cells studied with a monoclonal antibody against galactocerebroside. Proc Natl Acad Sci U S A 1982;79:2709–13.

35. Ramakrishnan H, Hedayati KK, Lullmann-Rauch R, Wessig C, Fewou SN, Maier H, et al. Increasing Sulfatide Synthesis in Myelin-Forming Cells of Arylsulfatase A-Deficient Mice Causes Demyelination and Neurological Symptoms Reminiscent of Human Metachromatic Leukodystrophy. J Neurosci 2007;27:9482–90.

36. Blomqvist M, Osterbye T, Månsson JE, Horn T, Buschard K, Fredman P. Sulfatide is associated with insulin granules and located to microdomains of a cultured beta cell line. Glycoconj J 2002;19:403–13.

37. Blomqvist M, Osterbye T, Månsson J-E, Horn T, Buschard K, Fredman P. Selective lack of the C16:0 fatty acid isoform of sulfatide in pancreas of type II diabetic animal models. APMIS 2003;111:867–77.

38. Buschard K, Blomqvist M, Osterbye T, Fredman P. Involvement of sulfatide in beta cells and type 1 and type 2 diabetes. Diabetologia 2005;48:1957–62.

39. Buschard K, Bracey AW, McElroy DL, Magis AT, Osterbye T, Atkinson MA, et al. Sulfatide Preserves Insulin Crystals Not by Being Integrated in the Lattice but by Stabilizing Their Surface. J Diabetes Res 2016;2016:1–5.

40. Merten M, Beythien C, Gutensohn K, Kuhnl P, Meinertz T, Thiagarajan P. Sulfatides activate platelets through P-selectin and enhance platelet and platelet-leukocyte aggregation. Arterioscler Thromb Vasc Biol 2005;25:258–63.

41. Garcia J, Callewaert N, Borsig L. P-selectin mediates metastatic progression through binding to sulfatides on tumor cells. Glycobiology

2007;17:185–96.

42. Zhang G, Nie H, Yang J, Ding X, Huang Y, Yu H, et al. Sulfatide-activated type II NKT cells prevent allergic airway inflammation by inhibiting type I NKT cell function in a mouse model of asthma. Am J Physiol Lung Cell Mol Physiol 2011;301:L975-84.

43. Sørensen JØ, Buschard K, Brogren C-H. The preventive role of type 2 NKT cells in the development of type 1 diabetes. APMIS 2014;122:167–82.

44. Yang SH, Lee JP, Jang HR, Cha R -h., Han SS, Jeon US, et al. Sulfatide-Reactive Natural Killer T Cells Abrogate Ischemia-Reperfusion Injury. J Am Soc Nephrol 2011;22:1305–14.

45. Maricic I, Sheng H, Marrero I, Seki E, Kisseleva T, Chaturvedi S, et al. Inhibition of type I natural killer T cells by retinoids or following sulfatide-mediated activation of type II natural killer T cells attenuates alcoholic liver disease in mice. Hepatology 2015;61:1357–69.

46. Kwiecinski J, Rhost S, Löfbom L, Blomqvist M, Månsson JE, Cardell SL, et al. Sulfatide attenuates experimental Staphylococcus aureus sepsis through a CD1d-dependent pathway. Infect Immun 2013;81:1114–20.

47. Jeon S-B, Yoon HJ, Park S-H, Kim I-H, Park EJ. Sulfatide, a major lipid component of myelin sheath, activates inflammatory responses as an endogenous stimulator in brain-resident immune cells. J Immunol 2008;181:8077–87.

48. Shrum B, Anantha R V., Xu SX, Donnelly M, Haeryfar SMM, McCormick JK, et al. A robust scoring system to evaluate sepsis severity in an animal model. BMC Res Notes 2014;7:1–11.

49. Chambers JW, LoGrasso P V. Mitochondrial c-Jun N-terminal Kinase (JNK) signaling initiates physiological changes resulting in amplification of reactive oxygen species generation. J Biol Chem 2011;286:16052–62.

50. Pattabiraman G, Murphy M, Agliano F, Karlinsey K, Medvedev AE. IRAK4 activity controls immune responses to intracellular bacteria Listeria monocytogenes and Mycobacterium smegmatis. J Leukoc Biol 2018;104:811–20.

51. Kulsantiwong P, Pudla M, Srisaowakarn C, Boondit J, Utaisincharoen P. Pam2CSK4 and Pam3CSK4 induce iNOS expression via TBK1 and MyD88 molecules in mouse macrophage cell line RAW264.7. Inflamm Res 2017;66:843–53.

52. Moore AS, Holzbaur ELF. Dynamic recruitment and activation of ALS-associated TBK1 with its target optineurin are required for efficient mitophagy. Proc Natl Acad Sci U S A 2016;113:E3349–58.

53. Crowley SD, Gurley SB, Herrera MJ, Ruiz P, Griffiths R, Kumar AP, et al. Angiotensin II causes hypertension and cardiac hypertrophy through its receptors in the kidney. Proc Natl Acad Sci U S A 2006;103:17985–90.

54. Balla A, Tóth DJ, Soltész-Katona E, Szakadáti G, Erdélyi LS, Várnai P, et al. Mapping of the localization of type 1 angiotensin receptor in membrane microdomains using bioluminescence resonance energy transfer-based sensors. J Biol Chem 2012;287:9090–9.

55. Kallikourdis M, Trovato AE, Roselli G, Muscolini M, Porciello N, Tuosto L, et al. Phosphatidylinositol 4-Phosphate 5-Kinase β Controls Recruitment of Lipid Rafts into the Immunological Synapse. J Immunol 2016:1501788.

56. Marwali MR, MacLeod MA, Muzia DN, Takei F. Lipid Rafts Mediate Association of LFA-1 and CD3 and Formation of the Immunological Synapse of CTL. J Immunol 2004;173:2960 LP – 2967.

57. Varshney P, Yadav V, Saini N. Lipid rafts in immune signalling: current progress and future perspective. Immunology 2016;149:13–24.

58. Zumerle S, Molon B, Viola A. Membrane Rafts in T Cell Activation: A Spotlight on CD28 Costimulation. Front Immunol 2017;8:1467.

59. Badenhoop K, Boehm BO. Genetic susceptibility and immunological synapse in type 1 diabetes and thyroid autoimmune disease. Exp Clin Endocrinol Diabetes 2004;112:407–15.

60. Rodríguez-Fernández JL. Antigen presentation by dendritic cells in rheumatoid arthritis. Curr Top Med Chem 2013;13:712–9.

61. Shapiro S, Galboiz Y, Lahat N, Kinarty A, Miller A. The "immunological-synapse" at its APC side in relapsing and secondary-progressive multiple sclerosis: modulation by interferon-beta. J Neuroimmunol 2003;144:116–24.

62. Kanter JL, Narayana S, Ho PP, Catz I, Warren KG, Sobel RA, et al. Lipid microarrays identify key mediators of autoimmune brain inflammation. Nat Med 2006;12:138–43.

63. Halmer R, Walter S, Faßbender K. Sphingolipids: Important players in multiple sclerosis. Cell Physiol Biochem 2014;34:111–8.

64. Sebode M, Wigger J, Filpe P, Fischer L, Weidemann S, Krech T, et al. Inflammatory phenotype of intrahepatic sulfatide-reactive type II NKT cells in humans with autoimmune hepatitis. Front Immunol 2019;10:1–14.

65. Wang SX, Yang CL, Zhang M, Zhang P, Liu RT, Zhang N, et al. Sulfatides ameliorate experimental autoimmune neuritis by suppressing Th1/Th17 cells. J Neuroimmunol 2019;326:55–61.

66. Novakova L, Singh AK, Axelsson M, Ståhlman M, Adiels M, Malmeström C, et al. Sulfatide isoform pattern in cerebrospinal fluid discriminates progressive MS from relapsing-remitting MS. J Neurochem 2018;146:322–32.

67. Isaac G, Pernber Z, Gieselmann V, Hansson E, Bergquist J, Månsson JE. Sulfatide with short fatty acid dominates in astrocytes and neurons. FEBS J 2006;273:1782–90.

68. Buschard K, Blomqvist M, Månsson JE, Fredman P, Juhl K, Gromada J. C16:0 Sulfatide inhibits insulin secretion in rat β-cells by reducing the sensitivity of KATP channels to ATP inhibition. Diabetes 2006;55:2826–34.
69. Blomqvist M, Carrier M, Andrews T, Pettersson K, Månsson JE, Rynmark BM, et al. In vivo administration of the C16:0 fatty acid isoform of sulfatide increases pancreatic sulfatide and enhances glucose-stimulated insulin secretion in Zucker fatty (fa/fa) rats. Diabetes Metab Res Rev 2005;21:158–66.

HMGB1 분비 억제를 통한 Sulfatide의 대식세포에서의 염증 억제 효과

< 지도교수 신 전 수 >

연세대학교 대학원 의과학과

김 희 수

High mobility group box 1 (HMGB1)은 패혈증 후반부에 나타나는 패혈증 중재 물질로 미토겐활성화단백질키나아제 (MAPK)와 NF-κB, 그리고 활성산소 (ROS)와 같은 경로를 통해 염증 시 분비되어 진다고 알려져 있다. Sulfatide는 HMGB1과 달리 myelin sheath에 다량 존재하는 스핑고지질로 면역학적 역할에 대한 의견이 분분하다. 중추신경계에서는 sulfatide가 염증을 일으킨다고 보고되었고, 반대로 말초면역계에서는 sulfatide가 세포를 보호하는 역할을 한다고 보고되었다. Sulfatide가 가지고 있는 면역학적 역할에 대한 이견을 말초면역계에서 확인하기 위해 sulfatide가 말초에서 보이는 면역학적 특징을 Raw 264.7 세포주가 sulfatide를 전/후처리와 LPS 자극을 주었을 때 분비하는 HMGB1양을 비교함으로써 연구해보고자 하였다. Sulfatide의 전처리와 후처리 모두 LPS 자극에 의한 HMGB1의 세포질로의 이동과 분비량이 줄어는 것을 확인하였으며, 톨유사수용체 4 (TLR4)의 하위 신호 전달 경로 분자인 c-Jun N-terminal kinase (JNK)의 인산화와 p65 분자의 핵내이동량이 감소하였다. LPS에 의한 활성산소 생성은 sulfatide의 전처리에 의해 줄었으며, 이는 IRAK4나 TBK1과 같은 활성체의 인산화가 감소하여 일어난 것임을 확인하였다. 상위 신호 전달 과정을 찾고자 지질 라프트 (lipid raft)를 연구하였다. 지질 라프트와 비오틴화 sulfatide가 공존하고, LPS 자극으로 인한 지질 라프트 내로 TLR4의 이동 역시 감소하였다. 이를 통해 전처치 된 sulfatide는 TLR4이 지질 라프트 내로 이동하는 것과 신호 전달을 방해하고, 그 결과로 소염 효과를 내는 것을 알 수 있었다. 한편, 후처치 된 sulfatide는 대사적 특징을 바꿈으로써 소염 효과를 내는 것 또한 확인 할 수 있었다. 실험쥐에서 LPS 매개 실험적 패혈증 모델에서도 sulfatide 처리로 인해 혈장 내 HMGB1, TNF-α, 그리고 IL-6의 수치가 낮아짐에 따라 생존율이 증가하고 패혈증 질병 척도 점수가 낮아짐을 확인하였다.

핵심되는 말 : Sulfatide, HMGB1, TLR4, 지질 라프트, 패혈증, NF-κB, 활성산소, 대사

PUBLICATION LIST

1. **Kim HS**, Han M, Park IH, Park CH, Kwak MS, et al. "Sulfatide Inhibits HMGB1 Secretion by Hindering Toll-Like Receptor 4 Localization Within Lipid Rafts", Frontiers in Immunology, 2020; 11:1305.

2. Kwak MS*, **Kim HS***, Lee B, Kim YH, Son M, Shin JS. "Immunological Significance of HMGB1 Post-Translational Modification and Redox Biology", Frontiers in Immunology, June 2020

3. Lee JJ, Park IH, Rhee WJ, **Kim HS**, Shin JS. "HMGB1 modulates the balance between senescence and apoptosis in response to genotoxic stress", FASEB Journal, October 2019

4. Kwak MS, **Kim HS**, Lkhamsuren K, Kim YH, Han M, Shin JM, *et al.*. "Peroxiredoxin-mediated disulfide bond formation is required for nucleocytoplasmic translocation and secretion of HMGB1 in response to inflammatory stimuli", Redox Biology, June 2019